Distributed Pressure and Temperature Sensing Based on Stimulated Brillouin Scattering

Jing Wang

Thesis submitted to the faculty of the Virginia Polytechnic Institute and State University in partial fulfillment of the requirements for the degree of

Master of Science

In

Electrical Engineering

Anbo Wang, Chair

Gary R.Pickrell

Yong Xu

December 1st, 2013

Blacksburg, Virginia

Keywords: distributed sensing pressure sensing, stimulated Brillouin scattering, distributed high temperature sensing

Distributed Pressure and Temperature Sensing Based on Stimulated Brillouin Scattering

Jing Wang

ABSTRACT

Brillouin scattering has been verified to be an effective mechanism in temperature and strain sensing. This kind of sensors can be applied to civil structural monitoring of pipelines, railroads, and other industries for disaster prevention. This thesis first presents a novel fiber sensing scheme for long-span fully-distributed pressure measurement based on Brillouin scattering in a side-hole fiber. After that, it demonstrates that Brillouin frequency keeps linear relation with temperature up to 1000℃; Brillouin scattering is a promising mechanism in high temperature distributed sensing.

A side-hole fiber has two longitudinal air holes in the fiber cladding. When a pressure is applied on the fiber, the two principal axes of the fiber birefringence yield different Brillouin frequency shifts in the Brillouin scattering. The differential Brillouin scattering continuously along the fiber thus permits distributed pressure measurement. Our sensor system was designed to analyze the Brillouin scattering in the two principal axes of a side-hole fiber in time domain. The developed system was tested under pressure from 0 to 10,000 psi for 100m and 600m side-hole fibers, respectively. Experimental results show fibers with side holes of different sizes possess different pressure sensitivities. The highest sensitivity of the measured pressure induced differential Brillouin frequency shift is 0.0012MHz/psi. The demonstrated spatial resolution is 2m, which maybe further improved by using shorter light pulses.

A traditional Brillouin optical time domain analysis BOTDA system was launched to test the relation between Brillouin frequency and temperature from room temperature to 1000℃ environment over 600m optical fiber. Our preliminary experimental results also demonstrated a

5m spatial resolution with 10 ℃ temperature resolution; these results may further be improved in the future.

Acknowledgements

I would like to express my gratitude and appreciation to my advisor Dr. Anbo Wang for his guidance, support in helping me to conduct and complete this work. I thank him for accepting me to study and collaborate in this excellent research group. I also would like to thank the other members of this group for their assistance.

I would like to thank my project manager Dr. Dorothy Wang for her patience, insight and extensive experience she shared with me. I would also like to thank Dr. Zhihao Yu for his support in my project.

In addition, I would also owe a lot of thanks to the staff and students of CPT. Very special thanks to Aram Lee, Nan Wu, Chaofan Wang, Li Yu, Lingmei Ma, Di Hu, Zhipeng Tian, Dr. Dong for their encouragement and friendship.

Finally, I would like to give my thanks to my family. My parents have always been supporting me and offering me endless inspiration and support. My brother has been sharing all my happiness and sorrows in my memory.

Table of Contents

List of Figures

List of Tables

1 Introduction

1.1 Motivation

Distributed temperature and pressure sensing is essential to maintaining safety and operational efficiency in complex industrial facilities and civil infrastructure. Installing single point sensors in different locations could realize quasi-distributed sensing, but the signal demodulation process is complicated and the installing process is labor consuming. In some special cases, such as pavement performance monitoring, pipeline leakage detection and oil recovery, continuous measurement in large scale is preferred. Duplicating single-point sensors would significantly increase the financial budget, even the installation process is labor intensive. Fully-distributed temperature and pressure sensing is essential to simplify the interrogation.

Optical fiber provides an ideal platform for distributed sensing because of its potential to form a low-cost, long-distance sensing system, and thus many researchers in the world participated in developing better optical fiber based distributed sensing. Currently, this technology is mainly based on scattering in optical fibers, such as Rayleigh scattering, Brillouin scattering, and Raman scattering. Despite their successes in many applications in structural health monitoring and industrial process control, they have inherently limited functionality.

Temperature sensing was only concentrated in relative low range, (less than 700 ℃); application in high temperature sensing (i.e. 1000 ℃) was performed by single point sensors. Strain was commonly investigated, but pressure sensing was not investigated fully.

In our group, we have investigated and demonstrated fully-distributed fiber-optic sensing technologies that could potentially fulfill the needs of distributed pressure measurement using a single optical fiber along hundreds of meters span. Also, we have demonstrated that Brillouin Scattering is a potential choice for realizing distributed high temperature (i.e. 1000 ℃) sensing along hundreds of meter span.

1.2 Optical fiber sensors

Optical fiber sensors, with the advantages of small size, low weight, immunity to electromagnetic interference, etc. have been applied to various sensing purposes such as temperature, pressure, gas sensing and so on. The development of optical instruments and components further extends their performance and stability.

There are four categories of optical sensors based on different sensing parameters: intensity modulation, wavelength modulation, polarization modulation and phase modulation.

1.2.1 Intensity-modulated sensors

In the initial stage of optical fiber sensor development, intensity-modulated sensors were widely used attribute their simplicity and low cost[1]. The sensing principle is that light intensity coupled to the sensor head is fluctuated with the parameter to be detected, i.e. pressure. Measurements were conducted by converting the light signal into electrical signal and by predicting the trend of temperature or pressure based on the electrical signal. Basic structure of an intensity-modulated sensor is to place a fiber straight, and launch high power into the fiber. When outer force is applied, the change in pressure is transmitted to the micro-bending on the fiber; light intensity received by the photodetector will vary in accordance with the applied force as shown in Figure 1.1[2]. Distributed sensing can be realized by launching a pulse beam instead of a continuous wave (cw) beam into the fiber. But pre-calibrating is required to eliminate errors induced by light source instability and fiber connections. One well-developed commercially available intensity-modulated sensor is the multi-mode optical fiber microbend sensor. The mechanical periodic microbend can couple the energy of guided modes in the fiber to radiation modes and thus attenuate transmitted light, the resolution of this sensor can be better than 0.1%. However, the power fluctuation of the optical source and the fiber loss limit its accuracy to a few percent of the full scale[3].

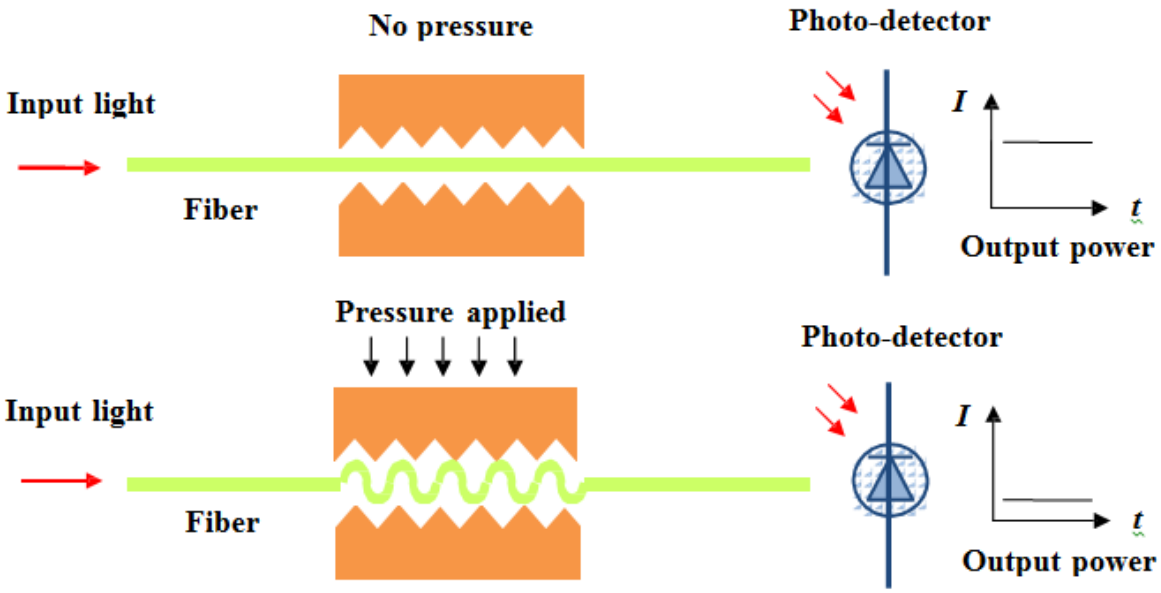

Figure 1.1 Intensity-modulated optical sensors[2] used under fair use, 2013

1.2.2 Wavelength-modulated sensors

Wavelength-modulated sensors take advantage of the light spectrum for sensing measurement. Broadband light spectrum is usually injected to interrogate the sensor. Extracting surrounding environment parameter is usually finished by comparing the amplitude at two or several fixed wavelength or continuous wavelength scanning. Fiber Bragg Gratings (FBGs) are one of the most widely used wavelength-modulated sensors in temperature monitoring, strain monitoring and civil engineering. Figure 1.2 illustrates one structure of FBG. The grating region is usually coated by elastic material or sealed in glass bubble; they can measure the hydrostatic pressure with high resolution. The fundamental principle for a FBG is that only the light at specific wavelength is reflected back when a broadband light is launched into the fiber. This wavelength, denoted as Bragg wavelength, is changing proportional with external environment, i.e. temperature. Sensing information can be mapped by continuous monitoring of the Bragg wavelength. FBG is preferred for its good reliability, intrinsic wavelength-encoded operation.

They can be multiplexed for quasi-distributed sensing networks. However, it is noticeable that the bandwidth of broad light source requirement might be an obstacle in some potential applications.

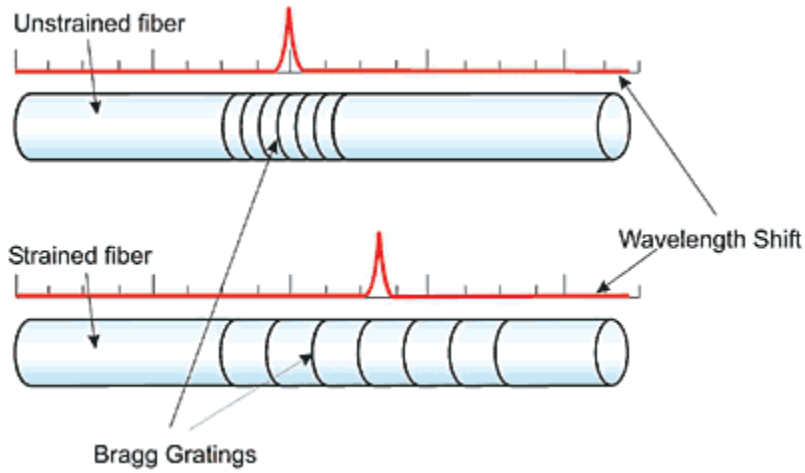

Figure 1.2 FBG for strain monitoring[4] used under fair use, 2013

1.2.3 Polarization-modulated sensors

As indicated by the definition, a polarization-modulated sensor works by monitoring the polarization of light to detect external environment perturbation, i.e. stress, strain. In a typical polarization-modulated sensing system, a linear polarized light is coupled at 45 degrees to the desired principle axes of a certain length of polarization-maintaining fiber (PMF). Figure 1.3 illustrates the principle of polarization-modulated sensors. Under external environment change, the phase difference between the two branches launched into two principle axes is varied. By analyzing the amplitude of detected signal the polarization information induced by external environment can be extracted, then stress or strain environment could be mapped. The drawback of polarization-modulated sensor is that it is hard to avoid the error induced by the random change in fiber birefringence.

Figure 1.3 illustration of polarization modulated sensor[2] used under fair use, 2013

1.2.4 Phase-modulated sensors

Phase-modulated sensor is utilizing the mechanism that optical phase of a beam passing through a fiber is modulated by the measurand[2]. Coherent laser source, who inject light beam into two fiber arms, is preferred in phase modulated sensors. High sensitive optical fiber sensors, such as Mach-Zehnder, Michelson, and Fabry-Perot sensors are widely used in industry. Mach-Zehnder and Michelson interferometers have been studied intensively for acoustic pressure monitoring in early stage of fiber optical sensing. However, these sensors require a very long length to obtain a desirable sensitivity due to the weak photoelastic effect or small stress-optic coefficients in optical fibers. Fabry-Perot interferometer (FPI) typically consists of two reflecting surfaces separated by a transparent plate. Interference will occur because of the multiple reflections between the two reflecting surfaces when a monochromatic light is injected into a Fabry-Perot cavity. Peaks and valleys in the interference spectrum indicate the constructive interference and destructive interference. Fabry-Perot cavity length, which changes in accordance with external environment parameter, can be interpreted by the demodulation of interference spectrum. Temperature or pressure information can be monitored by keep track of the change in Fabry-Perot cavity length[5]. This kind of sensor is robust; they can achieve high resolution and large dynamic change. But the time and labor consuming fabrication process is a flaw for this type of optical fiber sensor.

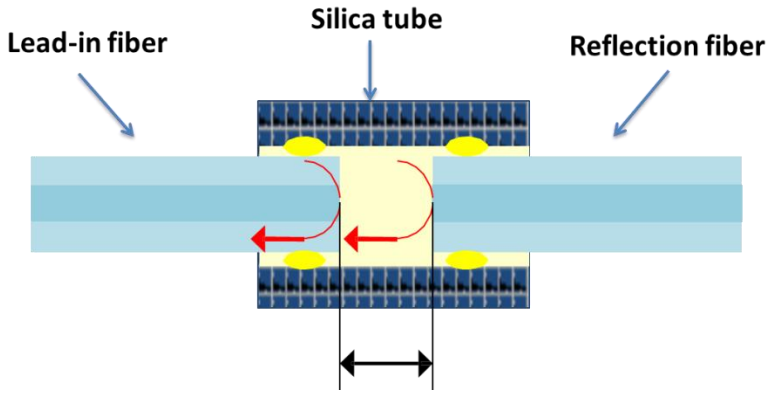

Figure 1.4 illustration of Fabry-Perot interderometer[2] used under fair use, 2013

1.3 Configuration of optical fiber sensors

Fiber sensors can be divided into three categories: single point sensor, qausi-distributed sensor and fully-distributed sensor. For a single point sensor, the sensing element is at the head of a fiber and the signal is guided and collected by an optical fiber. A quasi-distributed fiber-optic sensor is a system with a series of point sensors linked together to provide a number of specific and predetermined measurement points. A fully distributed sensor can detect desired information at any point along the fiber with a specific spatial resolution. It is also called an intrinsic distributed fiber-optic sensing.

1.3.1 Single point optical fiber sensor

Single point sensors are preferred when the interested parameter is only at one location or it is impossible to install several measurement points together. They are attractive due to their advantages of small size, harsh environment tolerance. Traditional sensors like thermometer, strain gauges, and down-hole oil temperature monitoring sensors are developed on single point sensing technique. Some new developed biosensors designed to work with small sensors are new direction for single point sensor. For a single point fiber sensor, the fiber head is usually working

as a probe and the light is collected and guided by the fiber. The interaction between the transducer, which is attached to the probe, generates an optical signal that can be translated into external environment information. One example is the optical fiber sensor attached with antibody that reacts with carcinogen benzopyrene (Bap) specifically; it can diagnose the cancer-causing agents in groundwater[6]. The fluorescence resulted from the interaction between antibody the Bap can be guided by optical fiber and further be diagnosed. But the drawbacks of single point fiber sensor is obvious, it is hard to acquire a series of information desired.

Figure 1.5 configuration of single point sensor

1.3.2 Quasi-distributed fiber-optic sensor

In a quasi-distributed fiber sensing system, a series of point sensors are linked together to provide a series of specific and predetermined measure points. These point sensors can share the same interrogation system and reduce the cost. Information is only extracted from locations at which point sensors are installed. Quasi-distributed sensors may be based on various kinds of theoretical principles, i.e. Fresnel reflection, Fabry-Perot interferometers, Fiber Bragg Gratings (FBG) and Long Period Gratings (LPG). They are attractive in civil engineering for monitor bridge or railway road damage. But these kind of low-cost sensors are not applicable to provide information at arbitrary location at certain spatial resolution. So fully distributed fiber optic sensors are preferred.

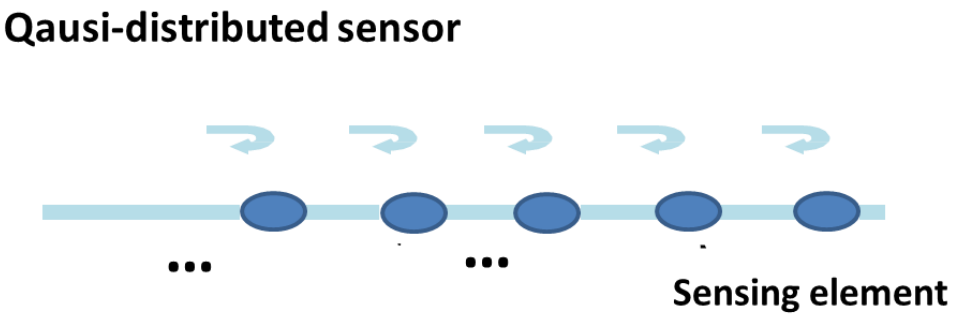

Figure 1.6 configuration of qausi-distributed sensor

1.3.3 Fully distributed fiber optic sensor

A fully distributed fiber optic sensing system can detect parameters at any location along the fiber with a desired spatial resolution. Distributed sensing is a technique unique to fiber optic sensing in the sense that almost no electrical cables could be converted to read through a time-domain reflectometer, nor do they have the ruggedness and flexibility of optical fiber sensors.

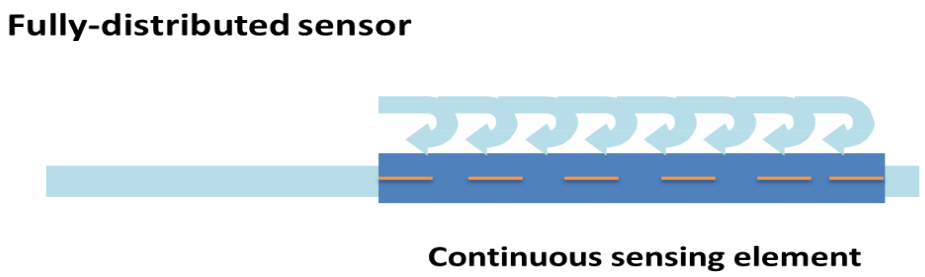

Figure 1.7 configuration of fully-distributed sensor

FDFS has gone through a long way and some are recognized as well-developed techniques, both technically and commercially. They are based on scattering, in which the scattered light in fiber is sensitive to the external measurand. Typical scatterings includes Rayleigh scattering, Brillouin scattering and Raman scattering. Brillouin scattering and Raman scattering are 20dB to 30dB weaker than Rayleigh scattering.

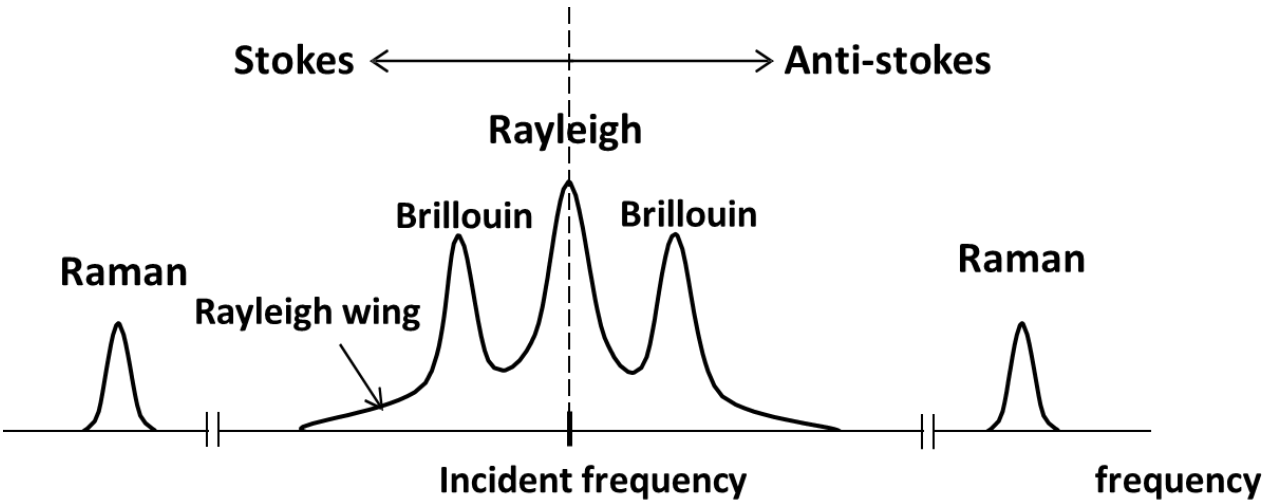

Figure 1.8 Typical scattering spectrum[7] used under fair use, 2013

Fully-distributed sensors used for monitoring temperature or pressure are usually founded on optical time domain reflectometry (OTDR) or optical frequency domain frequency reflectometry (OFDR). In an OTDR scheme, a pulse beam is injected into one end of the fiber and the backscattered light is collected by a photodetector. The detected pulse involves the external environment information to be monitored. While at the same time, location information can be calculated from the light speed propagating along the fiber. In an OFDR scheme, a cw wave or probe is split into two a reference arm and a measurement arm of an interferometer. Signal to be collected is the beating signal between reflection light and reference arm. In the demodulating process, the reflectivity as a function of length is acquired by retrieving Fourier transform. OFDR can achieve really high sensitivity.

Rayleigh scattering

Rayleigh scattering is caused by the elastic collision between the light wave and those small particles at much smaller wavelength than that of optical beam. It is one important kind of linear scattering, without frequency shift in scattered light. Rayleigh scattering accounts for the major attenuation in optical fibers. When coherent beam coupled into one end of the fiber, the intensity and polarization state of the back reflected scattered light contains the desired temperature or

strain information. Accomplishment of distributed temperature sensing was conducted by utilizing Rayleigh scattering coefficient of liquid-core and silica fiber[8]. Distributed strain sensing based on back-scattered Rayleigh scattering was reported by Froggatt using OFDR system[9]. More improved results were reported later. Fluctuation of light source, fiber bending loss or unexpected fiber bending loss may limit the sensitivity and accuracy of Rayleigh scattering based FDFS since they are relying on intensity and polarization diagonision as the sensing principle.

Raman scattering

Raman scattering is caused by thermally-induced molecular vibration of glass fiber. It is categorized as nonlinear scattering accompanied by a frequency shift of scattered light. The frequency shift is adequate with the characteristic vibration frequencies of the molecules. Photons scattered to higher frequencies are termed anti-Stokes components and those scattered to lower frequencies are called Stokes components. Particularly, only the intensity of anti-Stokes frequency component is an indicator of temperature environment. So, by calculating the ratio between anti-Stokes and Stokes component intensity, temperature information at the scattering point can be extracted. OTDR is used to map location information in Raman scattering. But the low Raman scattering coefficient, which is about three orders of magnitude weaker than that of Rayleigh scattering, low signal to noise ratio (SNR), makes the interrogation process complicated.

Brillouin scattering

Brillouin scattering is caused by the thermally excited acoustic vibration when a light beam is propagating along the fiber. It is also categorized as nonlinear scattering also accompanies with frequency shift in scattered light. The acoustic vibration enhances the energy flow from injected beam and scattering wave. The frequency difference decided by acoustic wave frequency is usually in the order of GHz and it varies in proportional with temperature or strain fluctuation. Spontaneous Brillouin scattering can happen with low requirement to input power, while SBS will occur above certain threshold. Compared with Raman scattering, Brillouin scattering are frequency detection and inherently more accurate and stable. Brillouin scattering based fiber

optic sensing has been a hot topic for the past two decades and significant results in temperature and strain were reported.

1.4 Summary and scope of research

Several techniques for distributed measurement by optical fibers have been demonstrated and further transitioned to industrial applications, including Fabry-Perot cavity sensors, FBGs, Raman optical time-domain reflectometry (ROTDR). However, the time and labor consuming fabrication process of Fabry-Perot cavity sensor, sophiscated signal processing algorithm restricted it from large amount production, it is not practical to install them for distributed sensing. Qausi-distributed FBGs can only realize the monitoring measurand information in fixed locations with fixed spatial resolution; it is not a flexible method if more requirements needed. To date, Brillouin scattering has been recognized to be an effective method for distributed temperature, strain and pressure sensing. Significant progress in spatial resolution, temperature resolution, and measurement length has been reported.

In this work, distributed transient pressure sensing based on BOTDA using side-hole fiber was reported; BOTDA has been demonstrated to be an effective and promising method for distributed high temperature sensing. This dissertation has been organized as following chapters:

Chapter 1 introduces the classification of optical fiber sensors, briefly reviews the distributed fiber optic sensors.

Chapter 2 discusses the structure of side-hole fiber, describes important parameters in side-hole fiber, the sensitivity of side-hole fiber. Specifically, the dimension and performance of side-hole fiber utilized in our work was presented.

Chapter 3 discusses the basic theory of stimulated Brillouin scattering, important parameters in Brillouin scattering, the theory foundation that supports Brillouin scattering as an effective method for distributed temperature, basic Brillouin scattering based measurement scheme and strain sensing and mathematical algorithm in BOTDA.

Chapter 4 first presents our work of distributed pressure sensing technique based on Brillouin scattering in a side-hole fiber. The differential Brillouin frequency shift gives an indication of the

applied pressure. Therefore, by measuring the Brillouin scattering distributedly along the fiber, fully distributed measurement of pressure can be realized.

In the second part, it presents our work in high temperature distributed sensing based on Brillouin scattering. Our work indicates linear relationship between Brillouin frequency and temperature maintains in high temperature environment (i.e. 1000 ℃).

Chapter 5 summarizes the contribution of this work and discusses the improvement of future research

2 Side-hole fiber

Side-hole fiber was proposed by Xie in 1986 and he demonstrated that side-hole fiber with widely tunable pressure-induced birefringence is a possible sensor for hydrostatic or acoustic pressure[10].

2.1 Important parameters of side-hole fiber

A typical single-mode fiber resembles the structure of PANDA fiber, but with two open channels in the place of the stress members[10], as shown in Figure 2.1.

Figure 2.1 structure of side-hole fiber

Side-hole fiber can be used as a pressure sensor. Stretching sensitivity, which depends on intrinsic and tension-induced modal birefringence, is the most important parameter in fabricating a pressure sensor. In elliptical jacket fiber, such as PANDA fiber, bow-tie fiber, the stretching sensitivity is investigated to be much more dependent on tension-induced modal birefringence than intrinsic modal birefringence[11]. Side-hole fiber has been demonstrated to be an effective pressure sensor due to the birefringence variance with external pressure applied.

Single mode fiber is not truly single-mode because it could support two degenerate modes that are polarized in two orthogonal directions. In ideal conditions, a mode excited in x-polarized direction would not couple to the orthogonal y-polarized state. In usual fibers, there always exists

mixture of two polarization states induced by small departures. Mathematically, the mode propagation constant β is slightly different for the modes polarized in and y directions. This property is denoted as modal birefringence. It could be expressed by a dimensionless parameter:

$$B_m = \frac{|\beta_x - \beta_y|}{k_0} = |n_x - n_y| \tag{2-1}$$

Where n_x and n_y are the modal refractive index for the two orthogonally polarized states.

Further, the period at which the two modes exchange their powers in a periodic rate as they propagate along the fiber, beat length can be expressed as

$$L_B = \frac{2\pi}{|\beta_x - \beta_y|} = \frac{\lambda}{B_m} \tag{2-2}$$

The axis along which the mode index is smaller is called fast axis since the group velocity is larger when propagating. For the same reason, the axis with larger mode index is so called slow axis.

The birefringence for typical side-hole fiber can be expressed in formula 2-3:

$$B_f = (n_x - n_y) = B_0 + S_0 P_0 + S_i P_i \tag{2-3}$$

Where n_x and n_y are the effective refractive index of the two perpendicular degenerate propagation modes in single-mode fiber. B_0 denotes the static birefringence resulted from thermal stress and core deformations. P_0 and P_i refer to the external applied and internal pressure, respectively. S_0 and S_i are external and internal pressure sensitivity. Side-hole fiber can realize pressure sensing by monitoring the trace of fiber birefringence.

Further, the fiber birefringence of side-hole fiber can be measured by Brillouin Scattering. The difference of Brillouin Frequency between two orthogonal degenerate modes can be expressed as

$$\Delta v_B = v_{Bx} - v_{By} = \frac{2V_A}{\lambda} B_f = \frac{2V_A}{\lambda}(B_0 + S_0 P_0 + S_i P_i) \tag{2-4}$$

Where v_{Bx} and v_{By} are the Brillouin Frequency of the two degenerated modes. By measuring the Brillouin Frequency difference between two degenerated modes, the external applied pressure along the sensing side-hole fiber could be mapped.

2.2 Side-hole fiber in pressure measurement

Even though the basic structure for a side-hole fiber is just one elliptical core with two air holes on both sides, different size and position of the air holes leads to different pressure sensitivity. J.R.Clowes[12] conducted series of simulation and experiments to investigate their influence: finite-element method (FEM) was launched to simulate and calculate the pressure sensitivity of the fibers; in the experiment, they built a whole setup, the pressure induced birefringence in the side-hole fiber sensor was remotely monitored by a matched low-coherence interferometer. All their experiments were conducted at low temperature to exclude the influence of drifts in fiber birefringence in high temperature environment. Their simulation and experimental results both proved that the fiber with large holes has greater pressure sensitivity than that with small holes separated at greater distance from the core[12].

When external hydraulic pressure being applied to the side-hole fiber surface; the stress distribution detected by the fiber core is anisotropic due to the anisotropic of fiber geometry. This anisotropic stress further exaggerates the fiber birefringence via the photoelastic effect of the fiber as the pressure gets larger. As mentioned above, the pressure sensitivity S_0 and S_i are the sensitivities for external and internal pressure on the fiber, respectively. To simplify the problem, one assumption is restricted: when the fiber ends are sealed, the pressure inside the side holes is ambient pressure and keeps constant with certain applied external pressure. Under such assumption, the internal pressure term can be included into the static birefringence term, B_0 as defined before.

$$\Delta v_B = v_{Bx} - v_{By} = \frac{2v_A}{\lambda} B_f = \frac{2v_A}{\lambda}\left(B_0 + S_0 P_0\right) \qquad (2\text{-}5)$$

Where B_0 is originated from two aspects: fiber geometrical structure, like elliptical core and temperature change (typically >1000 ℃) in the fabrication process, also called stress birefringence.

2.3 Parameter of customized side-hole fibers

The side-hole fibers in our project were fabricated by Stocker Yale Inc. Their specifications and parameters are listed below in Table 2.1.

Table 2.1 specification of the side-hole fiber

parameters	Sample#1	Sample#2
Length (m)	100	600
Fiber geometry (μm):2A 2B	62,55	62,55
Core diameter (μm): 2r	8	7
Hole geometry(μm): 2a 2b	20,17	22,19
Hole spacing (μm, edge-to-edge): 2d-2b	10	9
Mode field diameter @1330nm (μm)	9.2	7.64

Cross sections of the two spools of side-hole fibers are shown in Figure 2.2. The centered core sections are white due to the light transmission, and there are cracks on the cross section from the fiber cleaving. Also noticeable is that, different from regular commercial available fibers, the shapes of the fiber core, cladding and air holes are not perfectly elliptical. The oval shapes of the side-hole fiber were induced by the fabrication process. The side-holes in Sample #1 are slightly smaller, and farther to the core comparing with those in Sample #2.

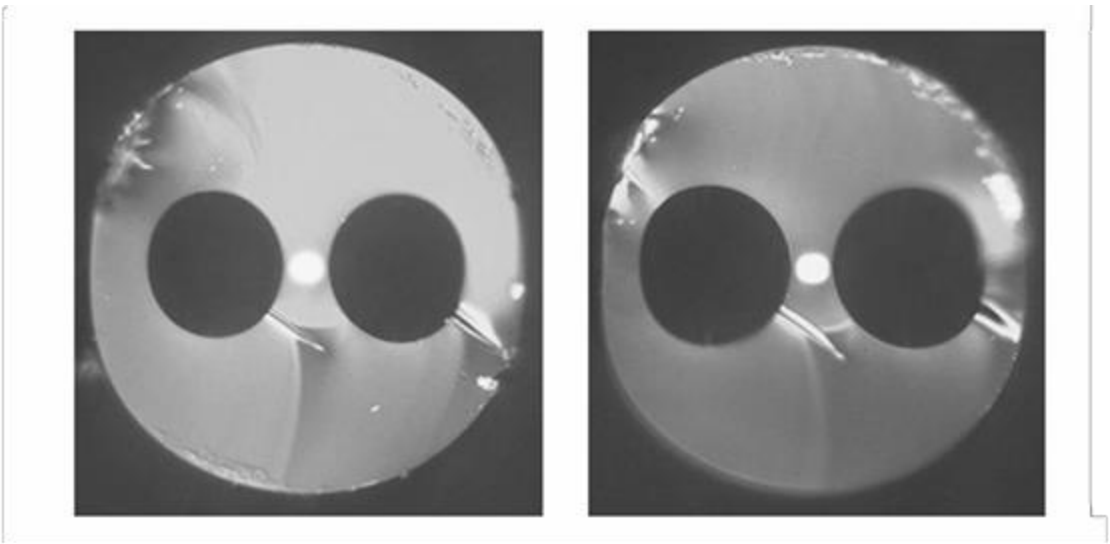

Figure 2.2 microscope photo of the cross section of side-hole fiber (left) sample #1; (right) sample #2

3 Brillouin Scattering in optical fiber

Brillouin Scattering, caused by the collective acoustic oscillations of the solid state matter[13], was first proposed in 1920s, but researchers first observed this nonlinear phenomenon in1964, with the advent of lasers; ever since, it has been studied extensively.

3.1 Classification of Brillouin Scattering

There are two kinds of Brillouin Scattering process in optical fibers, spontaneous Brillouin Scattering and Stimulated Brillouin Scattering (SBS). In spontaneous Brillouin Scattering, the light-scattering process is excited by thermal or by quantum-mechanical zero-point effects; the incident light does not modify the optical property of optical fibers. In contrast, the fluctuations in SBS are induced by the presence of the light field. SBS is typically much more efficient than the spontaneous Brillouin Scattering and is more widely adopted in distributed sensing technique.

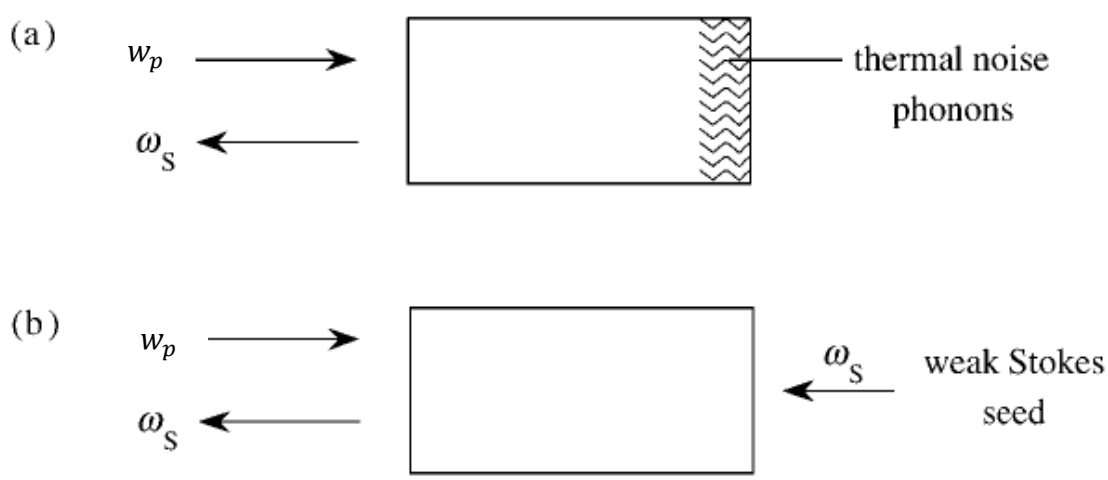

Figure 3.1 (a) SBS generator; (b) SBS amplifier[14] used under fair use, 2013

SBS can be described as a three-wave interaction, in which the pump, Stokes wave and acoustic wave reinforce each other. In Figure 3.1,ω_p and ω_s are the frequencies of pump beam and

Stokes wave. The frequency difference between two optical waves equals the induced acoustic wave frequency, namely, the Brillouin Frequency. In a SBS generator, only pump beam is externally applied, both the acoustic field and the Stokes field are stimulated from the thermal noise in the interaction region. It is initiated from spontaneous Brillouin Scattering. The incident pump and Stokes wave produce a beat signal at the Brillouin Frequency, which induces a density wave enhancing the acoustic wave and consequently increasing the number of phonons in the interacting region. This induces improved efficiency of the scattering process. SBS can be created when the pump power is above the threshold value. While in SBS amplifier, both pump and Stokes wave are applied externally. In practice, most distributed Brillouin Scattering based fiber sensing systems are designed based on SBS amplifier model.

3.2 Theoretical model of Stimulated Brillouin scattering

The process of SBS can be described classically as a nonlinear interaction between pump and Stokes field through an acoustic wave[15]. The pump field generates an acoustic wave through the process of electrostriction[16]. The travelling acoustic wave, which induces the periodic modulation refractive index of the fiber, can generate a periodic structure similar to Fiber Bragg Grating. This grating scatters the light through Bragg Diffraction. Due to the Doppler shift, the scattered light is downshifted in frequency with a magnitude of the acoustic frequency. During this scattering process, both the energy and the momentum must be conversed.

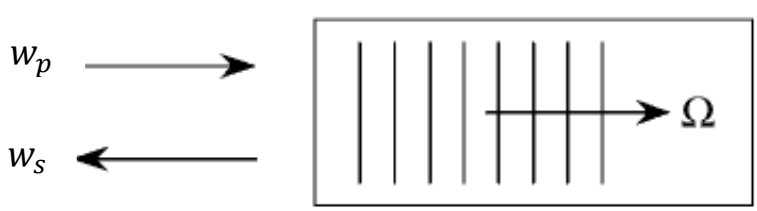

Figure 3.2 Stimulated Brillouin scattering

The frequencies and the wave vectors of the three waves are related by[15].

$$\Omega_B = \omega_p - \omega_s \qquad \overrightarrow{k_a} = \overrightarrow{k_p} - \overrightarrow{k_s}\,, \qquad (3\text{-}6)$$

Where ω_p and ω_s are the frequencies, k_p and k_s are the wave vectors of the pump and the Stokes waves, respectively. Ω_B and k_a are the frequency and wave vector of acoustic wave.

By taking the inner product of both sides of the equation yields

$$\begin{aligned} & k_p^2 + k_s^2 - 2k_p k_s \cos\theta_{p,s} = k_a^2 \\ & \Rightarrow k_p^2 + k_s^2 - 2k_p k_s + 4k_p k_s \sin^2\frac{\theta_{p,s}}{2} = k_a^2 \end{aligned} \qquad (3\text{-}7)$$

Where $\theta_{p,s}$ denotes the angle between $\overrightarrow{k_p} and\ \overrightarrow{k_s}$. The relation between wave velocity, wave frequency and wave vector is $w = vk$ for acoustic phonons, it manifests the proportionality between the angular frequency and wave number.

In the fact that $w_a \ll w_p, w_s$, it is commonly considered that $k_p \approx k_s$, combining $w_a = v_a k_a$, where v_a is the sound velocity, above equations evolves to

$$\begin{aligned} & 4k_p k_s \sin^2\frac{\theta_{p,s}}{2} = k_a^2 \\ & \Rightarrow 4k_p^2 v_a^2 \sin^2\frac{\theta_{p,s}}{2} = w_a^2 \\ & \Rightarrow \frac{2nv_a}{\lambda_p}\sin\frac{\theta_{p,s}}{2} = v_a \end{aligned} \qquad (3\text{-}8)$$

The common relation $\frac{2\pi}{\lambda_p} = \frac{w_p}{c}$ and $w_a = 2\pi v_a$ (λ_p stands for the wavelength of pump, and v_a stands for sound frequency) and light velocity in optical fiber $\frac{c}{n}$ are involved to derive the last step in the above equation.

From the above equation, it is easy to figure out that maximum frequency shift (v_a) occurs when the pump and stokes wave or as denoted, scattered light are in the opposite direction, (i.e. $\theta_{p,s} = \pi$). So the maximum frequency shift, Brillouin Frequency Shift, is then

$$v_B = \frac{2nv_a}{\lambda_p} \qquad (3\text{-}9)$$

Fibers with various parameters have different Brillouin Frequencies. A typical value of v_B for a standard Single Mode Fiber (SMF) is 12800 MHz at 1319nm and 10850 MHz at 1550nm[17-19] at room temperature.

The Brillouin Frequency was found to be linear with strain[20] and temperature[21], described as

$$\begin{aligned} v_B(T) &= v_B(T_r) + C_T(T - T_r) \\ v_B(\varepsilon) &= v_B(\varepsilon_r) + C_\varepsilon(\varepsilon - \varepsilon_r) \end{aligned} \qquad (3\text{-}10)$$

Where T is temperature; ε is tensile strain; T_r and ε_r are the reference temperature and strain, respectively; C_T and C_ε are temperature and strain coefficients. C_T and C_ε are believed to be constants, and was calibrated as $C_T = 1.10 \pm 0.02 MHz/K, C_\varepsilon = 0.0483 \pm 0.0004 MHz/\mu\varepsilon$ at 1550nm[22]. The Brillouin frequency dependencies on strain and temperature are induced by the acoustic velocity change in the fiber rather than refractive index change. From the above equation, we can get

$$\begin{aligned} C_T &= \frac{dv_B}{dT} = \frac{2n}{\lambda} \bullet \frac{dv_a}{dT} + \frac{2v_a}{\lambda} \bullet \frac{dn}{dT} \\ C_\varepsilon &= \frac{dv_B}{d\varepsilon} = \frac{2n}{\lambda} \bullet \frac{dv_a}{d\varepsilon} + \frac{2v_a}{\lambda} \bullet \frac{dn}{d\varepsilon} \end{aligned} \qquad (3\text{-}11)$$

Where the values of $dv_a/dT, dn/dT, dv_a/d\varepsilon, dn/d\varepsilon$ for silica fiber can be found in [23, 24] Table 3.1

Table 3.1 material coefficients of silica

	Strain $(1/\varepsilon)$	Temperature $(1/°C)$
v_a	5.4 (SAC)	$9.6 * 10^{-5}$ (TAC)
n	-0.20(SOC)	$0.5 * 10^{-6}$(TOC)

In the above table, SAC and SOC are denoted as strain acoustic coefficient and strain optical coefficient in optical fiber; TAC and TOC stands for temperature acoustic coefficient and temperature optical coefficient in a fiber. They can be expressed as

$$SAC = \frac{1}{v_a} \cdot \frac{dv_a}{d\varepsilon}$$
$$SOC = \frac{1}{n} \cdot \frac{dn}{d\varepsilon}$$
$$TAC = \frac{1}{v_a} \cdot \frac{dv_a}{dT}$$
$$TOC = \frac{1}{n} \cdot \frac{dn}{dT} \qquad (3\text{-}7)$$

It is obvious that the influence of temperature and strain to acoustic properties is dominant in optical fiber compared to that of fiber refractive index.

The growth of the Stokes wave is characterized by the Brillouin-gain spectrum peaking at $v = v_B$ since the amplification process only occurs in certain frequency range. Figure 3.3 shows a typical Brillouin gain spectrum in a single mode fiber. This spectrum may vary from Lorentzian to Gaussian profile if incident light power exceeds certain threshold. Another important parameter except for Brillouin Frequency in Brillouin gain spectrum is the linewidth of the spectrum, defined as Full Width at Half Maximum (FWHM). It is related to pulse duration if short pulses are applied to generate SBS. More recent measurements indicate that the Brillouin gain spectrum depends considerably on details of the fiber design and may contain multiple peaks that have their origins in different acoustic modes supported by the fiber[15].

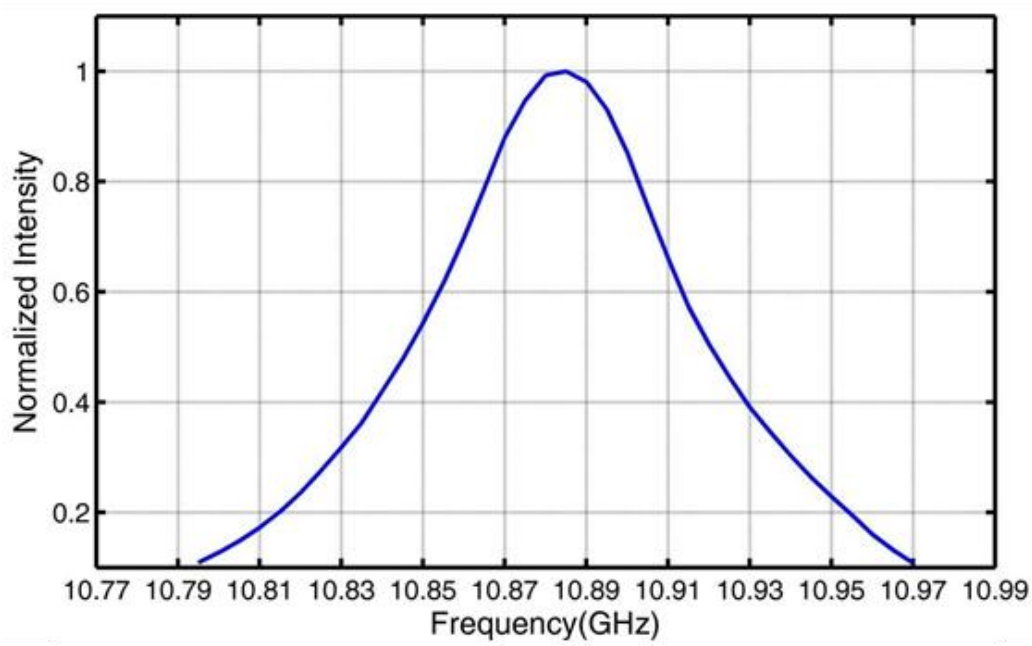

Figure 3.3 typical spectrum of a standard single-mode fiber

3.3 Brillouin gain and Brillouin loss Scheme

Brillouin scattering in fiber for optical sensing was first realized in 1989 and it was named Brillouin Optical Time Domain Analysis (BOTDA) by applying the pump-probe wave approach. In this basic model, a short pump pulse was injected into one end of the tested fiber and a cw probe beam was coupled into the other end. If the probe wave takes Stokes frequency, the energy couples from the pump to the Stokes wave, such the cw wave experiences Brillouin Gain process. If the probe wave is in anti-Stokes frequency, then the energy flows from the probe beam to pump pulse, and the detected is the Brillouin Loss spectrum of cw beam.

The gain or loss experienced by the cw beam, as a function of position along the fiber, can be determined by the time dependence of the detected cw light. In practical application, the time dependent cw signal is measured over a wide range of frequency differences between the pulse and cw beam. In such a way, the Brillouin Frequency at each fiber location could be recognized.

Based on the linear correlation between Brillouin Frequency and temperature (or strain), the temperature (or strain) distribution along the fiber can be extracted.

Brillouin Loss scheme was proposed to increase the sensing length compared to Brillouin gain structure. The cw beam is set at the anti-Stokes frequency rather than Stokes frequency, so the pulsed beam would experience gain while detected cw beam signal is Brillouin loss. The pulse signal switches from 'donor' to 'receiver' in energy flow process. As it is much harder to deplete the cw rather than a pulsed beam, longer sensing length can be achieved. A sensing length of 50 km with 5 m spatial resolution and 1 ℃ temperature resolution was reported using the Brillouin loss mechanism[13]. Long sensing length was not a dominant goal in our project, so BOTDA based gain scheme was applied in later experiment.

3.4 Basis of Signal Processing in SBS

The model of Brillouin scattering process uses the two coupled wave equations to describe the incident pulsed and cw laser intensities (I_p and I_{cw} $respectively$)[25] in steady state:

$$\frac{d}{dz}I_p = -gI_{cw}I_p - \alpha I_p$$
$$\frac{d}{dz}I_{cw} = -gI_{cw}I_p + \alpha I_{cw} \qquad (3\text{-}8)$$

Where $g = \dfrac{\gamma g_o \left(\Gamma_B / 2\right)^2}{\left[\Omega_B\left(T\right) - \Omega\right]^2 + \left(\Gamma_B / 2\right)^2}$

z stands for the distance from the pulsed laser end of the fiber, g_0 is the line center gain factor. Γ_B is the Brillouin linewidth, Ω is the frequency difference between the laser and $\Omega_B(T)$ is the temperature dependent Brillouin frequency shift. γ is a polarization factor, which accounts for the dependence of gain on the polarizations of the two beams[26].

It is noticeable that for pulse duration longer than phonon lifetime (10ns), these equations represent good approximation.

If g is taking positive sign, it stands for the process that pulse power couples to cw beam, as named Brillouin Gain Process; conversely, taking g in negative sign represents the process that cw beam power couples to pulsed beam, as defined Brillouin Loss Process. This sign is chosen based on the experiment whether the cw beam is up-shifted (g to be negative) or down-shifted (g to be negative).

Dr. Xiaoyi Bao proposed a perturbation method to solve for the Brillouin Gain in a particular location[27]. Their process can be explained below. cw beam can be expressed as following equation affected by fiber attenuation only:

$$I_{cw}(z) = I_{cw}(L)e^{-\alpha(L-z)} \tag{3-9}$$

Where $I_{cw}(L)$ represents the input power of the cw beam and L is the sensing length. Then pulsed wave can be expressed as

$$I_p(z) = I_p(0)\cdot\exp\left[-\frac{g\exp(-\alpha L)\left[\exp(\alpha z)-1\right]I_{cw}(L)}{\alpha}-\alpha z\right] \tag{3-12}$$

Where $I_p(0)$ is the input peak power of pulse beam.

Further substitute above equation into the original steady state equation (3-8) and integrate over distance u. u represents the distance pulsed beam interacts with cw beam; it is half the pulse length.

$$\int_{I_{cw}(z}^{I_{cw}(z+u)}\frac{dI_{cw}(z)}{dI_{cw}(z)} = \int_z^{z+u}\left(-gI_p(0)\exp[-\frac{gI_{cw}(L)e^{-\alpha L}\left(e^{\alpha z}-1\right)}{\alpha}-\alpha z]+\alpha\right)dz \tag{3-13}$$

Here, $z+u$ is the location in the fiber in which the leading edge of pulse meets the chosen wave front. Brillouin Gain information could be obtained by integrating over interaction length, from 0 to L as the pulsed beam travelling along the fiber.

Integration could be simplified by substituting

$$x = e^{\alpha z} \tag{3-14}$$

The results being

$$\int_{I_{cw}(z)}^{I_{cw}(z+u)} \frac{dI_{cw}(z)}{I_{cw}(z)} = \int_{e^{\alpha z}}^{e^{\alpha}(z+u)} -\frac{\kappa e^{-\beta(x-1)}}{\alpha x^2} dx - \alpha u \tag{3-15}$$

Where

$$\begin{aligned} \kappa &= gI_p(0) \\ \beta &= \frac{gI_{cw}(L)e^{-\alpha L}}{\alpha} \end{aligned} \tag{3-16}$$

The second order Exponential integral is defined as [28]

$$E_2(z_0) = \int_1^{\infty} \frac{\exp(-z_0 t)}{t^2} dt \tag{3-17}$$

By applying this formula to the integration, the gain of cw beam experienced due to the interaction with pulsed beam at position z is

$$\frac{I_{cw}(z)}{I_{cw}(z+u)} = \exp[K_0[\frac{E_2(\beta x_1)}{x_1} - \frac{E_2(\beta x_2)}{x_2}] - \alpha u] \tag{3-18}$$

Where

$$\begin{aligned} x_1 &= e^{\alpha z} \\ x_2 &= e^{\alpha(z+u)} \\ K_0 &= \frac{\kappa e^{\beta}}{\alpha} \end{aligned} \tag{3-19}$$

For Brillouin Gain case, above equation can be directly evaluated. But in Brillouin Loss case, a negative value of g leads to a negative value for the Exponential integral and it shows infinite integration value in formula 3-15 Fortunately, the difference in the two Exponential integrals in formula 3-16 is finite[27].

This theory founded the basement for the signal processing in SBS based distributed temperature and pressure sensing technique. Other improved technique were reported later by Aldo Minardo[29, 30]. Signal processing technique in centimeter spatial resolution was reported by Favien Ravet years later[31].

3.5 Polarization Effect in Brillouin Scattering

In Brillouin Scattering, interference occurs between two counter-propagating optical waves, inasmuch that signal is dependent on polarization states of the two beams.

A paper published by Deventer and Boot[32] explained the polarization behavior. Their study implies that in a fiber with varying linear and circular birefringence that is of sufficient length, the launched optical beam would pass through all points on the Poincare sphere with equal probability, the Brillouin gain will be no longer dependent on the injected polarization state of the two beams. Maximum gain is obtained when the launched polarizations are such that whenever the counter-propagating states are linear. In this case, at points in the fiber where the beams are in circular polarization states would not interfere. Minimum gain is obtained for the situation that two beams have perpendicular linear states and do not interfere. In this situation, positions at which two beams are in circular polarization states will interfere optimally[27].

This theory revealed that for maximum and minimum gain case, the corresponding polarization factor γ is $2/3$ and $1/3$ respectively. In most cases, maximum gain situation are designed to be achieved, hence the choice is $2/3$.

4 Distributed pressure and temperature measurement

Distributed pressure and temperature sensing was accomplished with our BOTDA system separately.

4.1 Distributed pressure measurement system

Brillouin scattering exits in the entire span of a fiber when both incident light beams are cw. In order to acquire location information and realized distributed measurement of Brillouin scattering, the incident light has to be modulated in intensity and frequency. Based on the type of the analysis domain, current Brillouin scattering based FDFS is mainly classified into three categories: time domain, frequency domain and correlation domain. Time domain analysis system is the most popular attribute to its better performance, and thus was adopted in our project.

4.1.1 Experiment system overview

The experimental system is shown in Figure 4.2 and Figure 4.3. A single-frequency narrow-linewidth laser is used as the light source; its output power is 54mW at 1550nm. With a 3dB coupler, the laser output is split into two paths for the probe and pump but their frequencies are intrinsically synchronized in this way.

Another noticeable feature in the system is that the light pulse was generated from the cw light by an electro-optic modulator (EOM). With the EOM2 set to high extinction ratio, electrical pulse generated from a signal generator which produces pulse in nanosecond pulsewidth can be modulated into optical pulses in same pulsewidth; after amplified by an EDFA, the pulse was sent into the fiber directly by circulator or coupler, as shown in Figure 4.2 and Figure 4.3. While for the cw beam, it is modulated by EOM1, which is driven by a tunable microwave generator. Both the polarization controller and microwave generator ensure largest modulation amplitude

from EOM. The tunable microwave generator also controls the frequency difference between the pulse and cw beam.

The EOM modulation creates sidebands in the laser spectrum, as marked by the red part in Figure 4.1. The upper sideband and fundamental frequency is not helpful to the stimulated Brillouin Scattering Gain process or even have negative effect. By adjusting the DC power supply of EOM and the polarization controller (PC), we could suppress the fundamental frequency amplitude to lowest value. After that, we set a big bandwidth for the tunable optical filter to get a sharp slope, so irrelevant component could be filtered out from the continuous wave as shown in Figure 4.1.

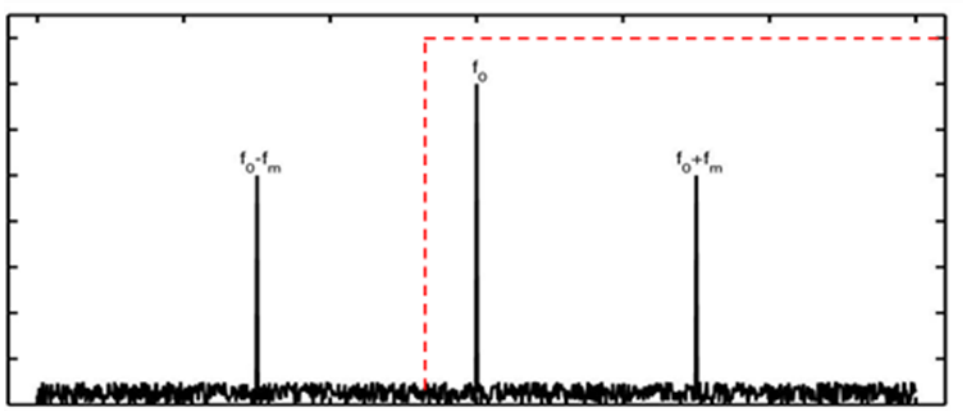

Figure 4.1 illustration of the optical spectrum of CW light after EOM modulation

There are slight differences between the operation in x axis and y axis due to some restrictions in the lab.

In the conduction of slow axis (x axis) experiment (shown in Figure 4.2), two polarization controllers, PC3 and PC4 are connected to the polarization beam splitters (PBS). All of our PBSs and polarization maintaining circulators are functional in slow axis, in such a way we could guarantee that both pulse and cw light launch into the slow axis of the side-hole fiber, which would maintain maximum Brillouin amplification along the fiber.

For the experiment in fast axis (y axis), PC3 is connected to a PM patchcord, and injected beam polarization state could be controlled by adjusting PC3(Figure 4.3). A polarization monitor

(TXP5016 PC controller) is used to monitor the beam polarization state outsourcing from the patchcord; we connect the patchcord to side-hole fiber when the beam polarization state aligns with the fast axis of PM patchcord. During the conduction, all the polarization sensitive parts are fixed on the table to insure a stable polarization state. The polarization state of injected pulse beam is controlled in a similar way, except a 9/1 coupler was fixed between PC4 and another PM patchcord; also, all the connections between PC4, 9/1 coupler and PM patchcord are fixed. The coupler ensures 90% of total pulse coupled into the side-hole fiber and 10% cw light received by photo detector. EDFA4 was inserted between the coupler and photo detector to improve signal quality.

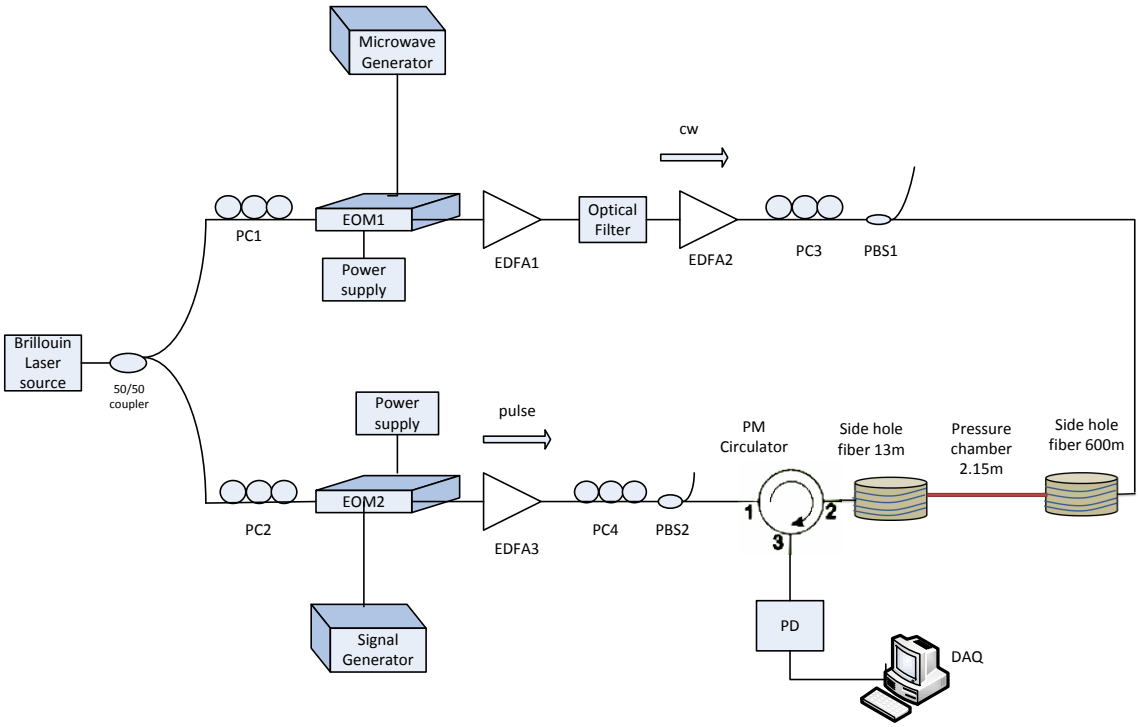

Figure 4.2 schematic of the slow axis setup

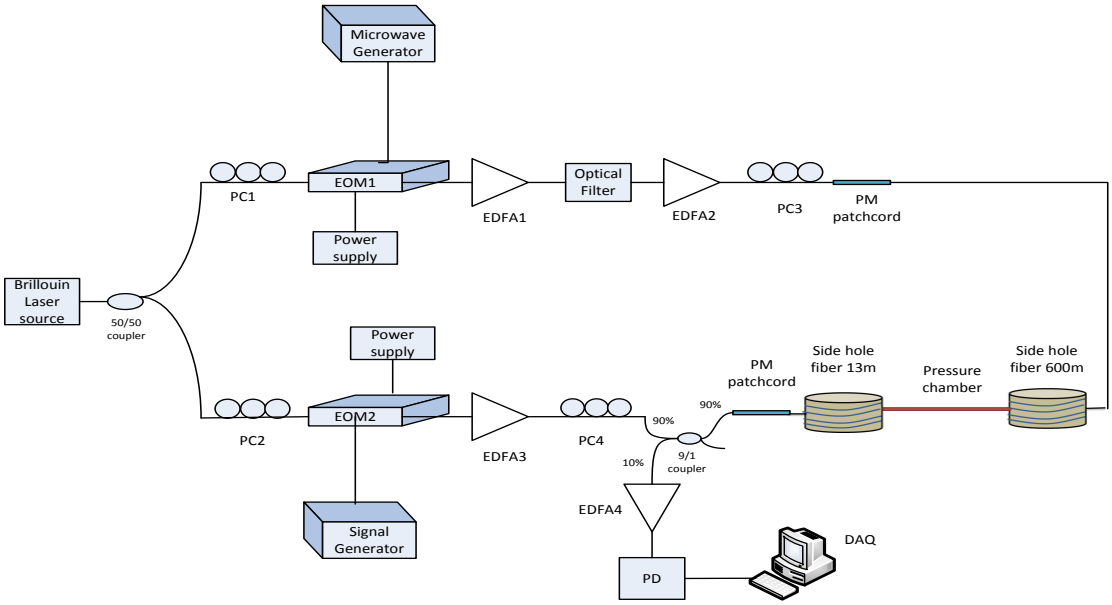

Figure 4.3 schematic of the fast axis setup

Figure 4.4 distributed pressure sensing experiment setup

4.1.2 Pressure loading chamber

In the experiment, a 2m side-hole fiber was sealed in a pressure chamber as shown in Figure 4.5. The applied pressure is provided by a pressure pump (MAXPRO, PP189), as shown in Figure 4.6. It is air driven with a drive air from 15 to 145 psi. The input air pressure is amplified into liquid pressure by a fixed pressure ratio based on the pressure intensifier principle. The pump has a large air piston joint to a smaller diameter plunger, and their area difference gives the pressure ratio which is 220 in our case. So the maximum outlet hydraulic pressure is 31900 psi.

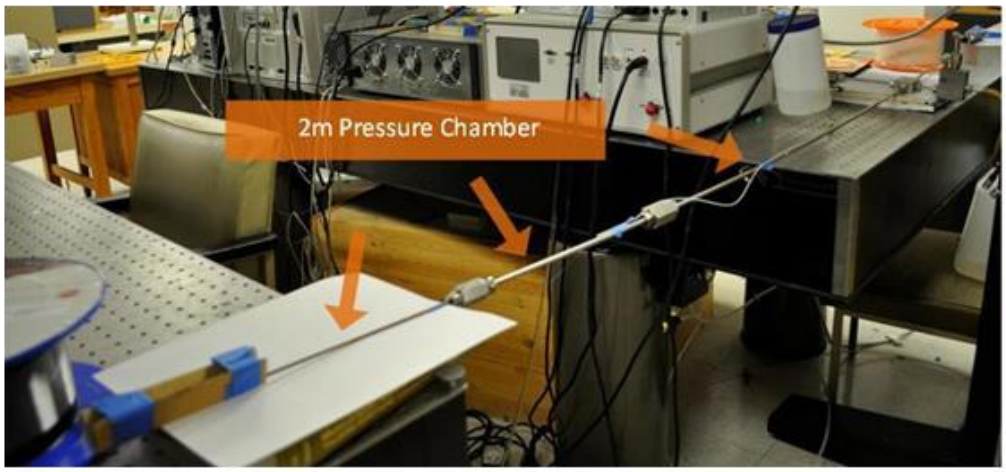

Figure 4.5 pressure loading chamber in the experiment

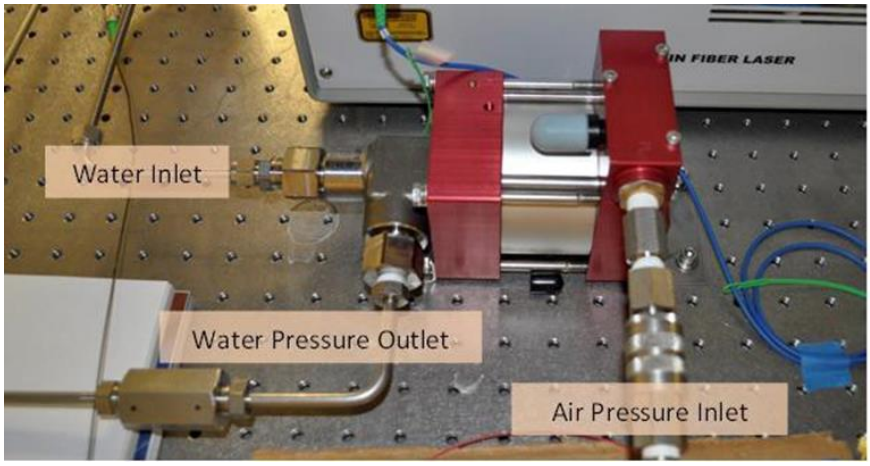

Figure 4.6 Air-to-liquid pressure pump

4.1.3 Experimental Results

The two spools of fabricated side-hole fiber were tested under different pressures; the pressures were applied on a fiber section of 2 meters with an increasing step about 1100psi. The system's polarization states were aligned to test the Brillouin frequencies in the two principal axes of the fiber separately. Figure 4.7 and Figure 4.8 show the two axis's Brillouin frequencies under different pressures.

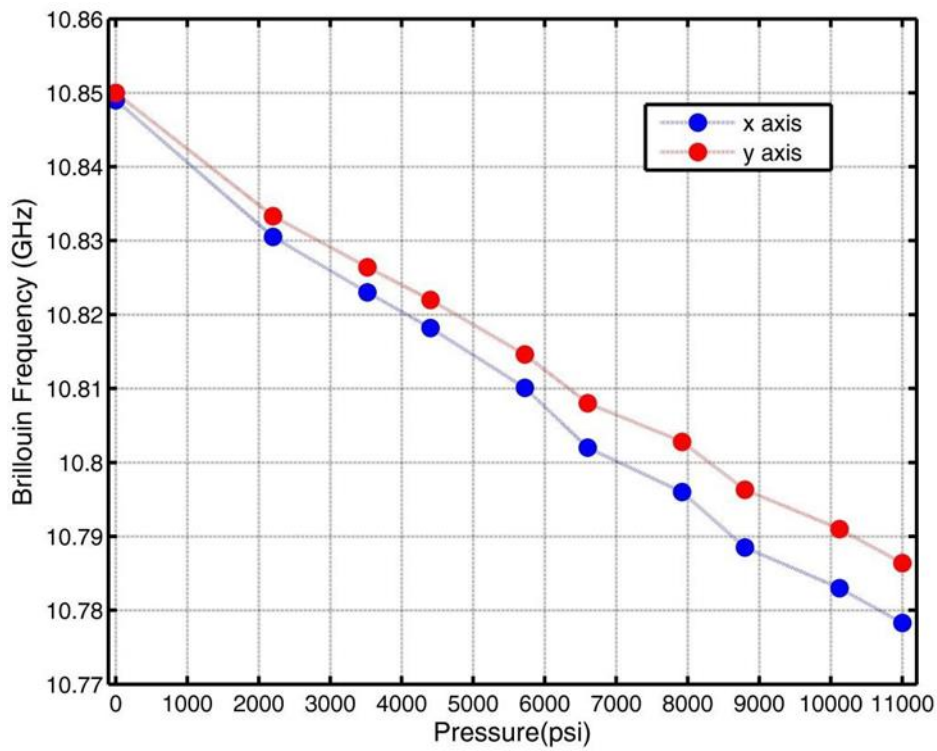

Figure 4.7 Brillouin frequency shift v.s. pressure for sample #1

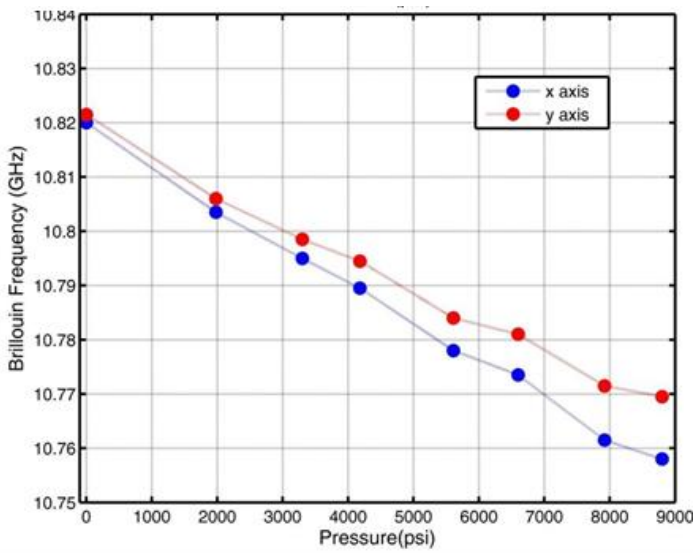

Figure 4.8 Brillouin frequency shift v.s. pressure for sample #2

From the experimental results we can see that for both fiber spools, the Brillouin frequency in y-axis is larger than that in x-axis, corresponding to larger effective refractive in y-axis. Therefore, we can have $\sigma_x < \sigma_y$ in formula 2-3. This is in good agreement with the simulation results as mentioned before, which indicates that the fast axis is x-axis for side-hole fibers. The differential Brillouin frequency between the two axes also changes with the applied pressure. The experimental results are shown in Figure 4.9 and Figure 4.10.

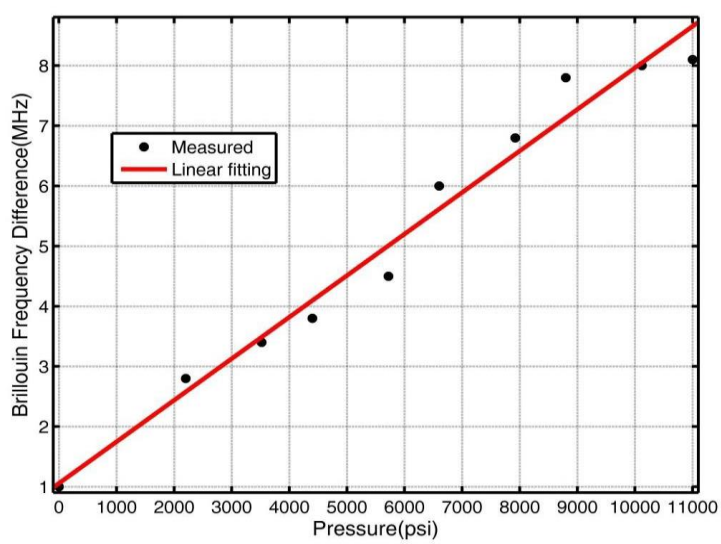

Figure 4.9 Differential Brillouin frequency v.s. pressure for sample #1

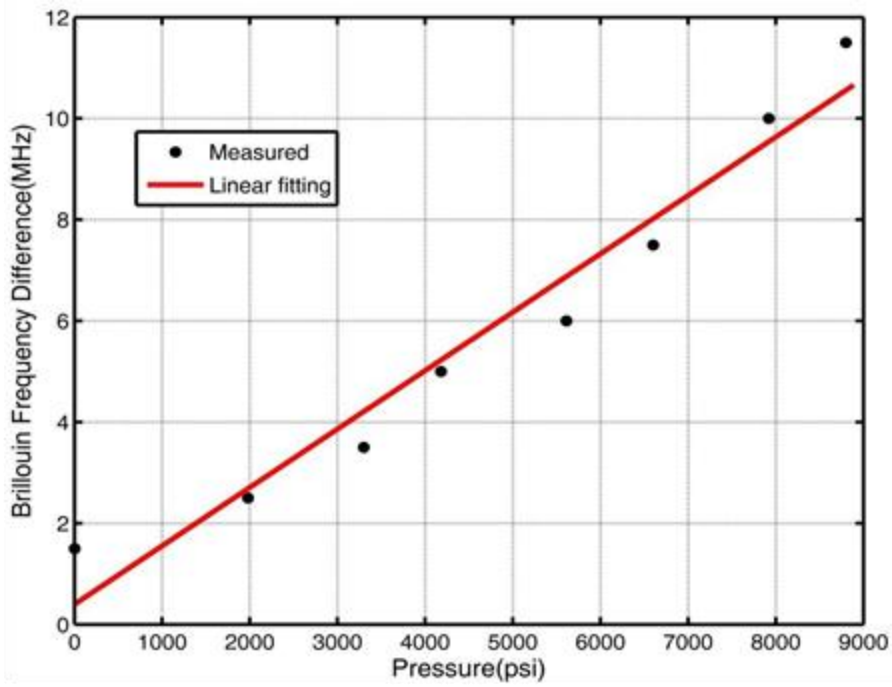

Figure 4.10 Differential Brillouin frequency v.s. pressure for sample #2

Based on the linear fitting of the experimental results, the pressure sensitivities of side-hole fiber sample #1 and #2 are 1.2×10^{-4} MHz/psi and 6.9×10^{-3} MHz/psi. From the comparison we can see that both of them present higher pressure sensitivity for sample #2 (red lines). This is in good agreement with the theoretical analysis which indicates that larger and closer side holes result in higher pressure sensitivities.

For both samples, the measured sensitivities are higher than simulations (simulation work was finished by Dr.Dorothy Wang). This is because of the strain induced from the Poisson effect, according to which the pressure of lateral stress can generate longitudinal strain. Unlike standard single-mode fiber which is isotropic, side-hole fiber is anisotropic in its cross section due to the air holes. Therefore, along the directions of the two principal axes, side-hole fiber has different equivalent values of Poisson's ratio and Young's modulus resulting in different pressure-induced longitudinal strains and thus different Brillouin frequency shifts. This means when there is pressure applied on the side-hole fiber, for each principal fiber axis, the total Brillouin frequency shift is contributed by two parts. One is directly from the compression stress, and the other is indirectly from the Poisson effect induced strain.

For the current sensing system, the differential Brillouin frequency measurement has 0.48MHz standard deviation for ten groups of data, as shown in Figure 4.11 with error bar plot.

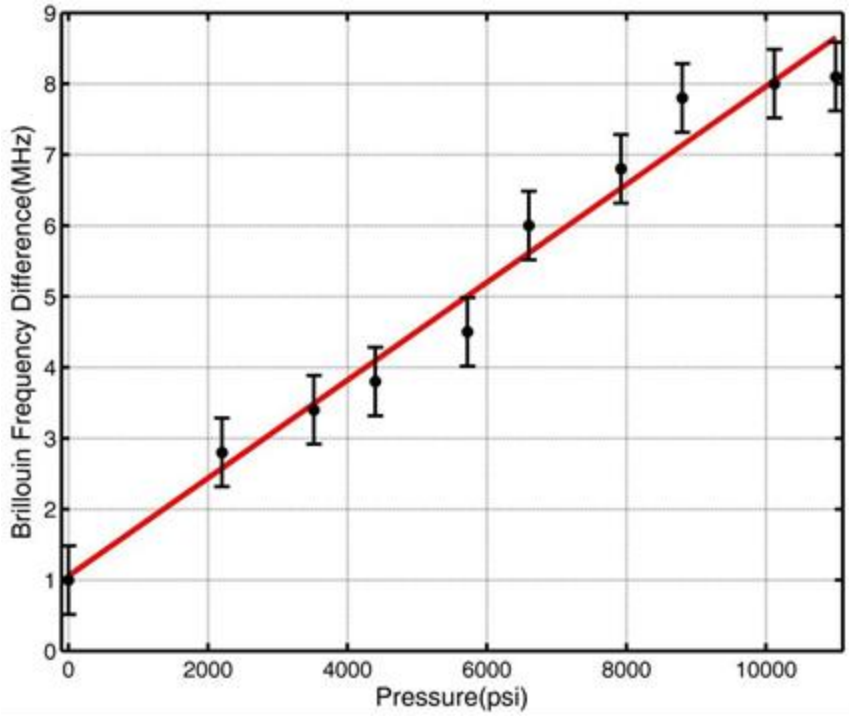

Figure 4.11 Measured pressure sensitivity for ample #2 with error bar plot

The fully-distributed measurement functionality is illustrated in Figure 4.12, which plots the Brillouin gain spectrum distribution profile along the fiber at different applied pressures. The figure clearly shows that the 2m pressurized fiber section has Brillouin gain spectrum at a different frequency region from the other fiber sections. And the spectrum is shifting towards lower frequencies as pressure increases.

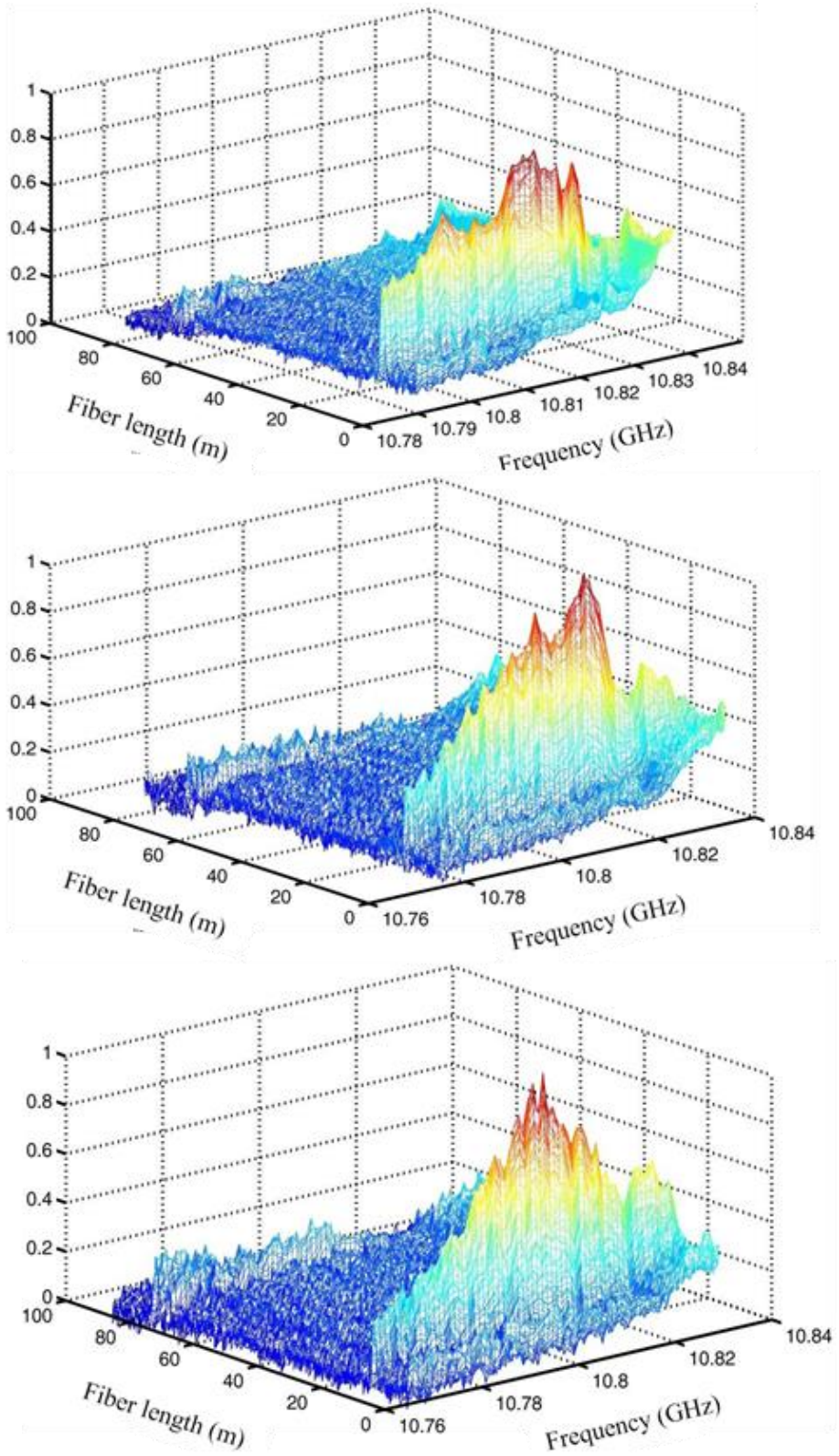

Figure 4.12 Brillouin gain spectrum distribution along sample #1 at 4400psi, 6600psi, 8800psi

4.2 Distributed high temperature sensing system

The objective of this project is to develop an advanced distributed sensing technology capable of monitoring refractory wear in an operating coal gasifier. This part presents some preliminary results of distributed high temperature sensing.

4.2.1 Experiment setup

The setup for high temperature distributed sensing was constructed quite similar with that of distributed pressure sensing. But side-hole fiber was replaced by regular single mode fiber, all the parts aimed at maintaining beam polarization state was removed. As shown in Figure 4.13. The pulse is sent into the tested fiber through a circulator after amplified by EDFA; for the cw light branch, after amplified by EDFA, a polarization scrambler was used to continuously change the polarization state of the pump in such a way to reduce the polarization noise in Stimulated Brillouin Scattering signal.

The process of tuning EOM and optical filter resembles the tips in distributed pressure sensing system.

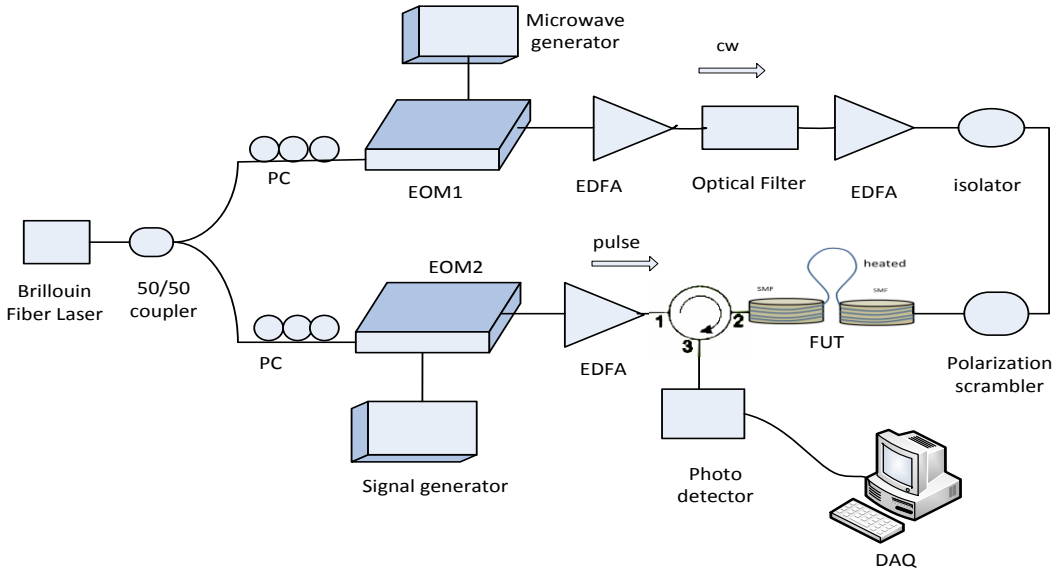

Figure 4.13 experiment setup for high temperature distributed sensing

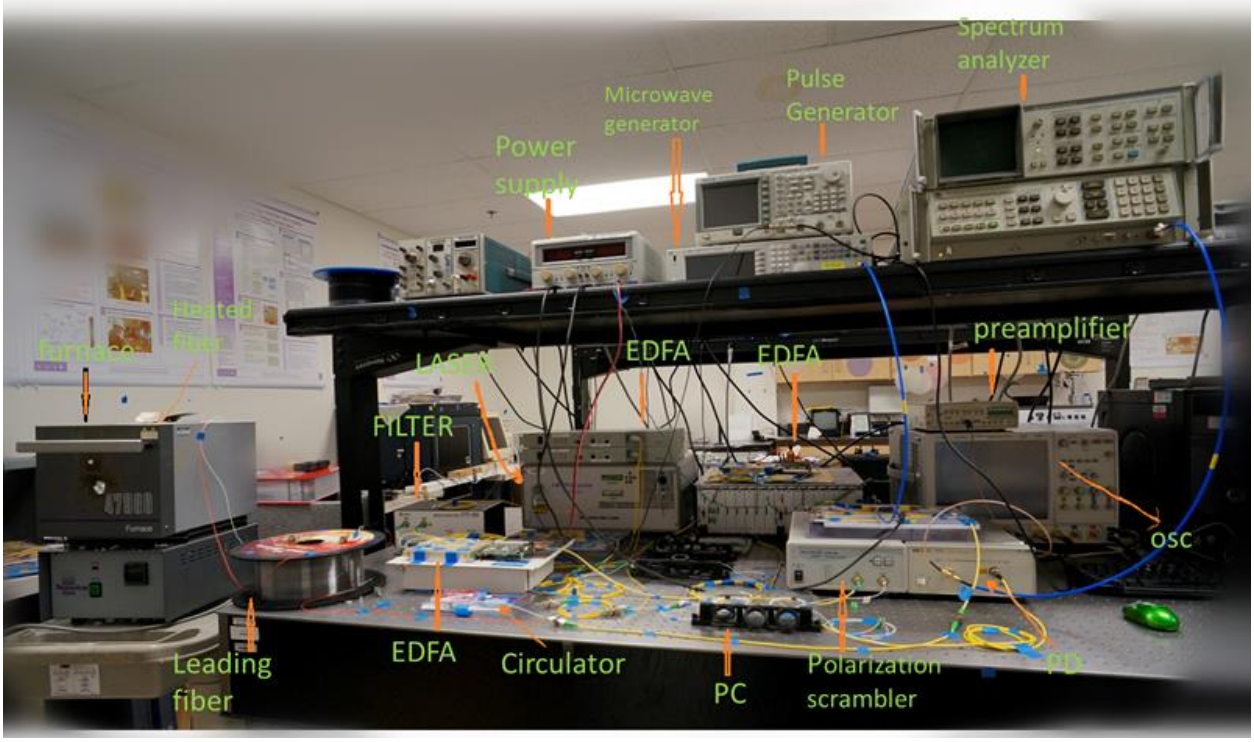

Figure 4.14 experiment setup

4.2.2 Experiment Results

To test stimulated Brillouin scattering in high temperature, an arbitrary 20m part long fiber in the middle of a 500m fiber spool was heated; pulsewidth 200ns which corresponds to 20m spatial resolution was picked. The heated fiber part was looped in 10cm diameter circle in a furnace; furnace temperature was set at 500 ℃ and 1000 ℃ respectively. A thermal couple was inserted into the furnace to monitor the temperature stability inside the furnace. Experiment data were acquired after the furnace temperature got stable.

Our results indicate that high temperature environment does not swallow stimulated Brillouin scattering process. Location information and Brillouin frequency of heated part can be mapped easily. As shown in Figure 4.15, tested results shows the Brillouin frequency of single mode fiber is 10.87GHz, but flows to around 11.3GHz and 11.67GHz respectively in 500 ℃ and 1000 ℃ environment.

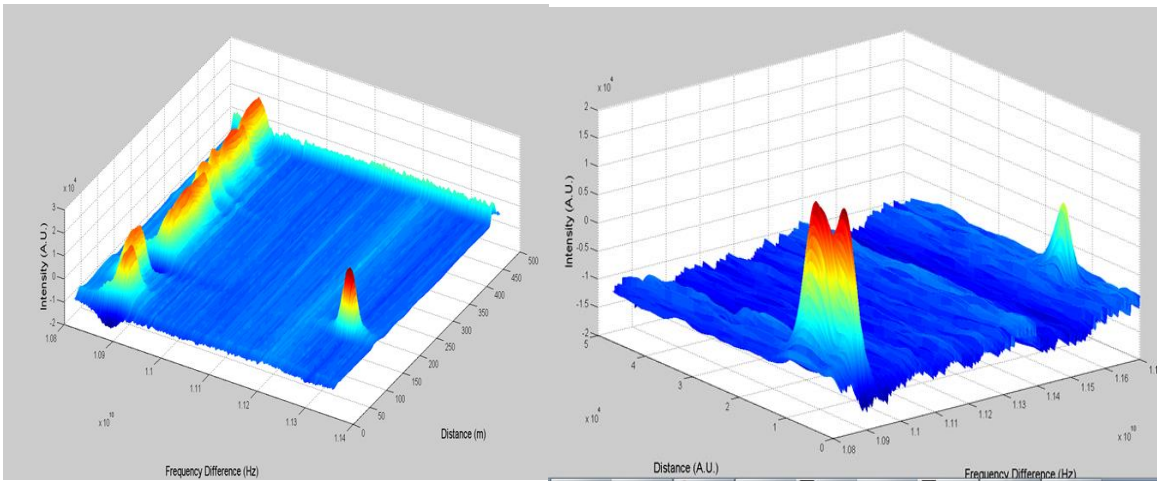

Figure 4.15 measurement result at 500°C and 1000°C

The non-uniformity of Brillouin frequency for fiber part placed in room temperature can be attributed to the non-uniform strain along the fiber. Since the fiber was rerouted manually, internal strain along the fiber could vary from part to part. Fortunately, this is a fixed pattern. Further experiment was launched to the same spool of fiber, except that heated section was removed, as shown in Figure 4.16. Comparing this result with the unheated fiber part shown above, we found obvious resemblance. Noticeable fact is that for the heated fiber part, temperature information was only included in the frequency information, this non-uniformity in room temperature does not really give negative effect on experiment principle.

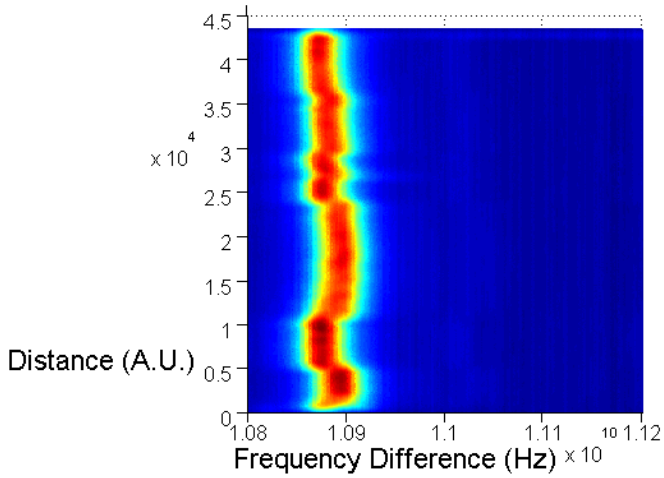

Figure 4.16 experiment result in room temperature

By subtracting the non-uniformity from the original Figure 4.16, a corrected result can be given in Figure 4.17.

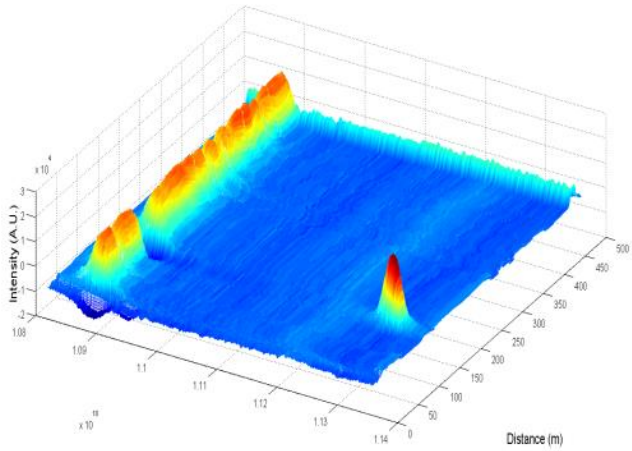

Figure 4.17 corrected results

Our system had been further tested as a robust distributed high temperature sensing system. An arbitrary 10m part of 500m optical fiber was heated, and we detected cw wave intensity vs. frequency difference between pulse and cw light along the fiber. Brillouin frequency shift of heated part shows a good linearity with temperature from 100 ℃ to 1000 ℃, as shown in Figure 4.18. This encouraging result implied that Stimulated Brillouin Scattering is a reliable method for high temperature distributed sensing.

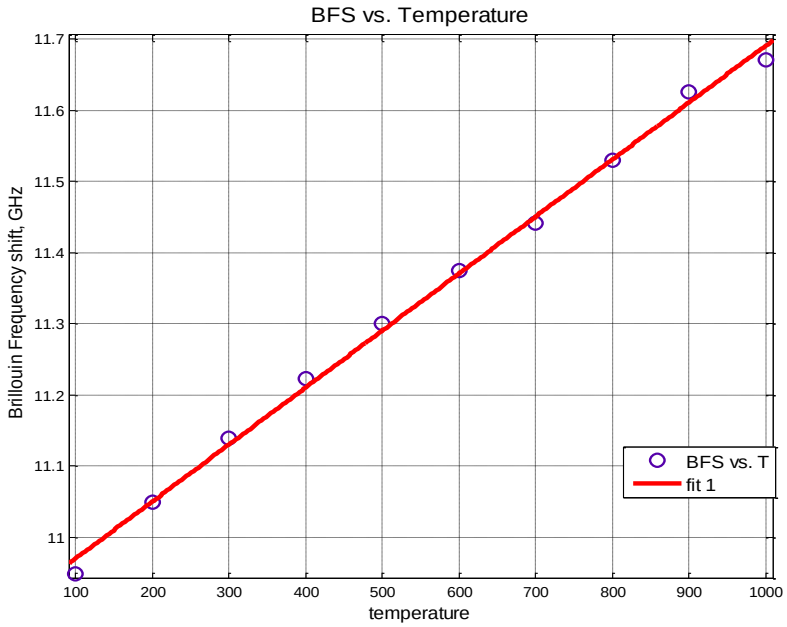

Figure 4.18 Brillouin frequency v.s. temperature

For better spatial resolution and temperature accuracy, similar experiment was operated with 50ns pulsewidth, which corresponds to 5m spatial resolution. 10m fiber part in the middle of 500m fiber spool was heated up to 980 ℃, 990 ℃ and 1000 ℃ respectively. At each temperature, the frequency difference between cw and pulse was swept from 11.6GHz to 11.72GHz with 1MHz step, and cw light intensity was recorded. The spectral shift as a function of temperature is evident from Figure 4.19.

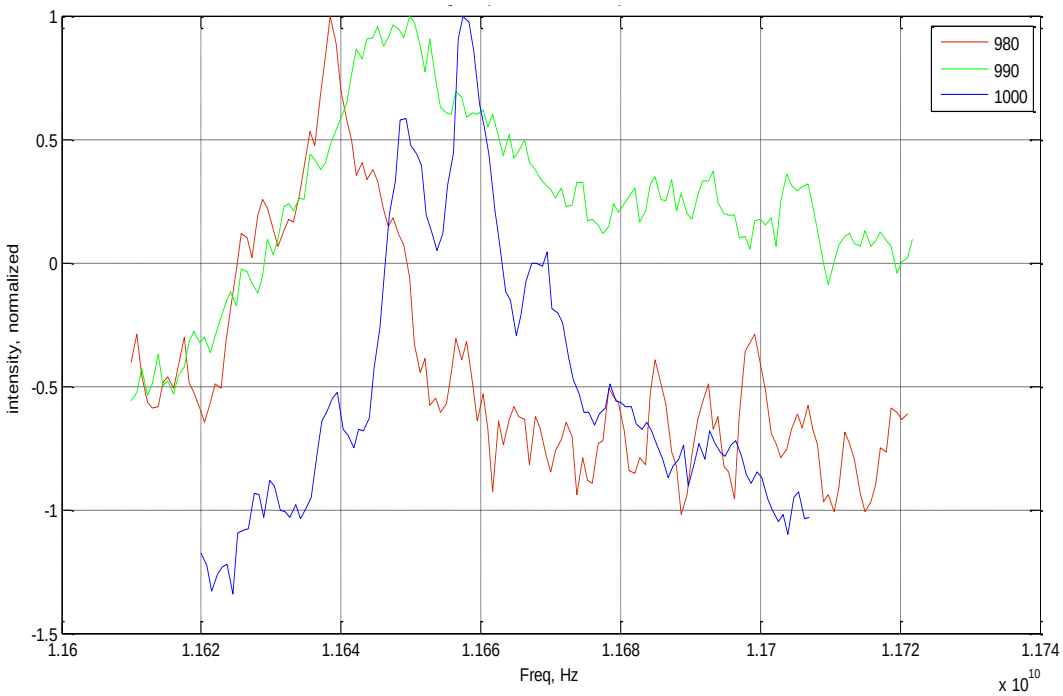

Figure 4.19 spectrum of a 5m fiber under 980°C(red), 990°C(green) and 1000°C (blue) respectively

5 Conclusion

This thesis presents the research of a stimulated Brillouin scattering based pressure and temperature sensing technique. In this chapter a summary of the completed tasks and a recommended paths for future study are provided.

We proposed and developed a fully-distributed pressure/transverse stress sensing technique based on Brillouin scattering in a side-hole fiber. The side-hole fiber is high birefringence single-mode fiber, with two longitudinal open air holes in the cladding region. The applied pressure on the side-hole fiber increases the fiber birefringence, resulting in different Brillouin frequency shifts along the two principal axes of the fiber. The differential Brillouin frequency shift gives an indication of the applied pressure. Therefore, by measuring the Brillouin scattering distributedly along the fiber, fully-distributed measurement of pressure can be realized.

The sensing system is designed based on BOTDA, which uses a pulsed light as the pump light and a CW light as the probe light. The frequency difference between them is scanned around the Brillouin frequency of the fiber. After scanning, the local Brillouin spectrum can be reconstructed, and the position information is given by the time delay from launching the pulse to its reaching at the interaction region with the CW light. The Brillouin frequencies along the two principal axes of the fiber are measured separately. Therefore, the polarization state in the system needs to be well maintained.

The birefringence of side-hole fiber changes with the pressure applied to side-hole fiber due to the two air holes, which break the geometric symmetry of the fiber.

Two spools of side-hole fiber (100m and 600m) were fabricated and tested in the sensing system under different hydraulic pressures from 0 to 10,000 psi. Experimental results show that fibers with side holes of different sizes possess different pressure sensitivities. Fibers with larger and closer side holes have higher pressure sensitivities. The measured pressure sensitivities of the two side-hole fiber spools are $6.9\times10^{-3} MHz/psi$ and $0.0012 MHz/psi$. The demonstrated spatial resolution is 2m, which can be further improved by using shorter light pulses.

With a similar BOTDA system and reconstruction of Brillouin spectrum of a single mode fiber, it indicates that Brillouin frequency keeps linear relation with temperature till 1000℃ environment. Experiments were launched by heating certain part of a 600m single mode fiber in a furnace and keeping other parts in room temperature. Our preliminary experimental results also demonstrated a 5m spatial resolution with 10℃ temperature. These results may further be improved in the future.

Reference

1. Chester, A., S.maartellucci and A.Scheggi, optical fiber sensors, 1967. **Nijhoff**.
2. Wang, Y., *A quasi-distributed sensing network based on wavelength-scanning time-division multiplexed fiber bragg grating.* phd thesis 2012.
3. Berthold, J.W., *historical review of microbend fiber-optic sensors.* Lightwave Technol, 1995. **13(7)**: p. 1193-1199.
4. Department of Electrical & Computer Engineering, B.Y.U., http://www.photonics.byu.edu/fbg.phtml.
5. Choi, H.S., H.F.Taylor, C.E.Lee, *high performance fiber optic temperature sensor using low-coherence interferometry.* optical society of America, 1997.
6. Jacobson, K.B., *ONRL Center for Biotechnology [Online] Avilable: http://web.ornl.gov/info/ornlreview/rev29_3/text/biosens.htm.* Biosensors and other medical and environmental probes.
7. Internet, http://www.omnisens.com/ditest/362-bst.php.
8. Hartog, A., *A distributed temperature sensor based on liquid-core optical fibers.* Lightwave Technol, 1983. **1(3)**: p. 498-509.
9. Froggatt, M.E., *calculation of birefringence in a waveguide based on Rayleigh scatter.* Google Patents, 2008.
10. H.M.Xie, p.D., and R.Ulrich, *Side-hole fiber for fiber-optic pressure sensing* optics letters, 1986. **11, No.5**
11. Satoshi Tanaka, K.Y., Seiichiro Kinugasa and Yoshihiro Ohtsuka *Birefringent Side-hole Fiber for Use in strain Sensor* optical review, 1997. **4, No.1A**
12. J.R.Clowes, S.S., and M.N.Zervas, *pressure sensitivity of side-hole optical fiber sensors.* IEEE Photon Technol Lett, 1998. **10**.
13. Xiaoyi bao, l.c., *Recent Progress in Distributed Fiber Optic Sensors.* Sensors, 2012.
14. www.knovel.com, E.R.f., chapter 9: Stimulated Brillouin and Stimulated Rayleigh Scattering p. 429-470.
15. P.Agrawal, G., *Nonlinear fiber optics 4th edition*
16. R.W.Shelby, *Nonlinear Optics* Academic Press 2003.
17. Horiguchi T, S.K., Kurashima T, Tateda M and Koyamada, *Tensile Strain dependence of Brillouin frequency shift in silica optical fibers.* Photonics Technology Letters, IEEE, 1989. **1(5)**: p. 2.
18. Smith, J., et al., *Simultaneous distributed strain and temperature measurement* Applied Optics, 1999. **38(25)**.
19. Farahani, M.A.a.T.G., *spontaneous raman scattering in optical fibers with modulated probe light for distributed temperature Raman remote sensing* journal of lightwave technology, 1999. **17(8)**.

20. T.Kurashima, T.H., and M.Tateda *Distributed-Temperature Sensing Using Stimulated Brillouin Scattering in Optical Silica Fibers.* Optical letters

15, 1990.

21. T.Horiguchi, T.K., M.Tateda, *Development of a Distributed Sensing Technique Using Brillouin Scattering* jouranal of lightwave technology, 1995. **13(7)**.
22. Parker , T., et al, *A fully distributed simultaneous strain and temperature sensor using spontaneous Brillouin backscatter* Photonics Technology Letters, IEEE, 1997. **9(7)**.
23. Law, P.C., et al, *Acoustic coefficients of P₂O<sub>5<sub>-doped silica fiber: acoustic velocity acoustic attenuation, and thermo-acoustic coefficient* Optical Materials Express, 2011. **1(4)**: p. 686-699.
24. Brown, D.C.a.H.J.H., *Thermal, stress, and thermo-optic effects in high average power double-clad silica fiber lasers* Quantum Electronics, IEEE Journal of 2001. **37(2)**: p. 207-217.
25. G.P.Agrawal, Nonlinear Fiber Opitcs, 1989: p. 268.
26. Chomsky, N., *What is Special About Language?*, in *SBS Lecture Series: Noam Chomsky*2012, University of Arizona.
27. X. Bao, J.D., Nicol Heron, David J. Webb, and D. A. Jackson, *Ecperimental and Theoretical Studies on a Distributed Temperature Sensor Based on Brillouin Scattering* journal of lightwave technology, 1995. **13**.
28. I.Stegun, M.A.a., *Handbook of Mathematical Functions.* Dover, 1965: p. 228-269.
29. Romeo Bernini, A.M., Luigi Zeni *reconstruction technique for stimulated Brillouin scattering distributed fiber-optic sensors* optical enginiiering 2002. **41**.
30. Aldo Minardo, R.B., Luigi Zeni, Luc Thevenaz and Favien Briffod, *A resconstruction technique for long-range stimulated Brillouin scattering distributed fiber-optic sensors: experimental results* Measurement Science & Technology, 2005. **16**: p. 900-908.
31. Fabien Favet, X.B., Yun Li, Quinrong Yu, Alexandre Yale, Vladimir P.Kalosha, and Liang Chen *Signal processing technique for distributed brillouin sensing at centimeter spatial resolution* jouranal of lightwave technology, 2007. **25**(11).
32. S.C.Rashleigh, *Origins and control of polarization effects in single mode fibers.* J.Lightw Technol, 1983. **LT-1**: p. 312-331.